Available online at www.sciencedirect.com
SCIENCE DIRECT®
Journal of Computational Physics 209 (2005) 226–248
JOURNAL OF COMPUTATIONAL PHYSICS
www.elsevier.com/locate/jcp

High-order linear multistep methods with general monotonicity and boundedness properties

Steven J. Ruuth [a,*], Willem Hundsdorfer [b]

[a] Department of Mathematics, Simon Fraser University, Burnaby, BC, Canada V5A 1S6
[b] CWI, P.O. Box 94079, 1090 GB Amsterdam, The Netherlands

Received 4 June 2004; received in revised form 30 November 2004; accepted 13 February 2005
Available online 23 May 2005

Abstract

We consider linear multistep methods that possess general monotonicity and boundedness properties. Strict monotonicity, in terms of arbitrary starting values for the multistep schemes, is only valid for a small class of methods, under very stringent step size restrictions. This makes them uncompetitive with the strong-stability-preserving (SSP) Runge–Kutta methods. By relaxing these strict monotonicity requirements a larger class of methods can be considered, including many methods of practical interest.

In this paper we construct linear multistep methods of high-order (up to six) that possess relaxed monotonicity or boundedness properties with optimal step size conditions. Numerical experiments show that the new schemes perform much better than the classical monotonicity-preserving multistep schemes. Moreover there is a substantial gain in efficiency compared to recently constructed SSP Runge–Kutta (SSPRK) methods.

MSC: 65L06; 65M06; 65M20; 35L65; 76M20

Keywords: Multistep schemes; Monotonicity; Strong stability; SSP; TVD; TVB

1. Introduction

Along with the usual linear stability and consistency requirements, non-linear monotonicity and boundedness properties are often desirable, and in particular they are frequently needed in the time discretization

* Corresponding author.
E-mail addresses: sruuth@sfu.ca (S.J. Ruuth), willem.hundsdorfer@cwi.nl (W. Hundsdorfer).

0021-9991/$ - see front matter © 2005 Elsevier Inc. All rights reserved.
doi:10.1016/j.jcp.2005.02.029

of PDEs with non-smooth solutions. In this paper we shall be concerned with systems of ordinary differential equations (ODEs) in $\mathbb{R}^m$,

$$w'(t) = F(w(t)), \quad w(0) = w_0, \tag{1}$$

that arise from the semi-discretization of (hyperbolic) partial differential equations (PDEs). We shall assume that there is a maximal step size $\Delta t_{\mathrm{FE}} > 0$ such that

$$\|v + \Delta t F(v)\| \leqslant \|v\| \quad \text{for all } 0 < \Delta t \leqslant \Delta t_{\mathrm{FE}}, \ \ v \in \mathbb{R}^m, \tag{2}$$

where $\|\cdot\|$ is a given semi-norm, such as the total variation over the components. We are interested in the discrete preservation of monotonicity and boundedness properties by numerical approximations $w_n \approx w(t_n)$, $t_n = n\Delta t$, generated by linear multistep methods. Of course, with the forward Euler method (2) leads to

$$\|w_n\| \leqslant \|w_0\| \quad \text{for all } n \geqslant 1, \tag{3}$$

whenever the step size restriction $\Delta t \leqslant \Delta t_{\mathrm{FE}}$ is valid. With higher-order linear multistep methods, we shall see that related monotonicity or boundedness properties can also arise, albeit with a (possibly) modified time step restriction.

We shall mainly consider explicit linear multistep methods

$$w_n = \sum_{j=1}^{k} (a_j w_{n-j} + b_j \Delta t F(w_{n-j})), \quad n \geqslant k, \tag{4}$$

where the starting vectors $w_0, w_1, \ldots, w_{k-1}$ are either given or computed by an appropriate starting procedure. A common generalization of (3) for multistep methods is

$$\|w_n\| \leqslant \max_{0 \leqslant j \leqslant k-1} \|w_j\|. \tag{5}$$

However, this property is only valid for a small class of methods under stringent step size restrictions; see Section 2 for a brief review.

It was shown in [7] that methods of practical relevance can be included in the theory if we consider multistep methods in combination with starting procedures that generate $w_1, w_2, \ldots, w_{k-1}$ from w_0. Instead of (5) we will consider the property

$$\|w_n\| \leqslant M\|w_0\| \quad \text{for all } n \geqslant 1, \tag{6}$$

where the size of the constant $M \geqslant 1$ will be determined by the starting procedure. In case $M = 1$, this will be referred to as *monotonicity*. If $M \geqslant 1$ this is a boundedness property. Following [7] we can determine constants C_{LM} such that (6) holds under the step size restriction $\Delta t \leqslant C_{\mathrm{LM}} \Delta t_{\mathrm{FE}}$.

The main application of such monotonicity and boundedness results are found in the numerical solution of hyperbolic PDEs, in particular for conservation laws. For such problems, the step size restriction $\Delta t \leqslant C_{\mathrm{LM}} \Delta t_{\mathrm{FE}}$ is often called a CFL condition and the threshold C_{LM} is then the CFL coefficient. For the one-dimensional equation

$$u_t + f(u)_x = 0, \tag{7}$$

spatial discretization will lead to a system of ODEs where the components of $w(t)$ approximate the PDE solution at grid points or surrounding cells, $w_i(t) \approx u(x_i, t)$. The discrete total variation $\|v\| = \mathrm{TV}(v)$ is a semi-norm defined as $\mathrm{TV}(v) = \sum_i |v_i - v_{i-1}|$, where, e.g. $v_0 = v_m$ for problems with periodic boundary conditions. For this semi-norm, the property (2) is called the TVD (total variation diminishing) property, and its generalization (6) with $M \geqslant 1$ is called the TVB (total variation bounded) property. This boundedness property is important because conservative TVB schemes are known [4] to converge to the correct entropy solutions of hyperbolic conservation laws.

In a previous paper [7] property (6) and the step size restriction $\Delta t \leqslant C_{\mathrm{LM}}\Delta t_{\mathrm{FE}}$ was studied for a class of second-order multistep schemes as well as the third- and fourth-order explicit Adams and extrapolated BDF schemes. In this paper, a more systematic study of high-order methods is carried out, leading to methods that satisfy the boundedness property (6) with optimal threshold factors C_{LM}. In particular, third- and fourth-order schemes are constructed that give 38% and 115% improvements in C_{LM} over the best schemes presented in [7]. This paper also gives the first studies of the boundedness property (6) and the corresponding step size restrictions for fifth- and sixth-order schemes.

A variety of theoretical results for general multistep schemes are presented in a related paper [6]. In particular, that paper proves that the boundedness property (6) arises when properties (2), (17) and (18) hold and a Runge–Kutta starting procedure is used. Generalizations of this result are also derived, including one that relaxes assumption (2). It is also shown that over the class of implicit linear multistep methods, the optimal threshold factors are (rather strictly) bounded according to $C_{\mathrm{LM}} \leqslant 2$ for orders $p \geqslant 2$, making such methods unattractive if the boundedness property (6) is crucial. In this paper we shall mainly be concerned with the construction of optimal explicit high-order schemes, and for precise theoretical details we shall refer to [6].

Numerical tests on some scalar conservation laws will show that our new optimal multistep methods are superior to the optimal schemes of [3,14,19] that satisfy (5).

Up to now, most of the effort to construct time step methods with optimal monotonicity properties has been directed to Runge–Kutta methods. Therefore, in our experiments also monotone SSP Runge–Kutta (SSPRK) methods of [10,16,20,21] will be taken into consideration. The examples provided in this paper demonstrate that our new multistep schemes are often more efficient (in terms of CPU) than standard SSPRK methods. They also have the advantage that they do not degrade accuracy near inflow boundaries of the PDE domain. On the other hand, our methods require more storage than popular SSPRK methods. See Remark 4.1 for further details on these last two points.

In Section 2, a brief review is presented of multistep methods satisfying the strict monotonicity property (5), including some improvements on the methods listed in [3]. The main section of this paper is Section 3, where optimal methods satisfying (6) with order $p = 3, 4, 5, 6$ and step number $k = p$ or $k = p + 1$ will be constructed. Numerical illustrations are given in Section 4. There we consider a monotonicity test for the linear advection equation with first-order upwind spatial discretization, as well as a comparison of the accuracy for various multistep and Runge–Kutta methods applied to Burgers' equation with high-order ENO spatial discretizations. The final Section 5 contains a summary and conclusions.

2. Monotonicity with arbitrary starting values

2.1. Methods with non-negative coefficients

Assume that all $a_j, b_j \geqslant 0$. By regarding the step (4) as a linear combination of scaled forward Euler steps it easily follows that the monotonicity property (5) will be valid under (2) with the step size restriction

$$\Delta t \leqslant K_{\mathrm{LM}}\Delta t_{\mathrm{FE}}, \qquad K_{\mathrm{LM}} = \min_{1\leqslant j\leqslant k} \frac{a_j}{b_j} \quad \text{if } a_j, b_j \geqslant 0 \text{ for all } j, \tag{8}$$

with convention $0/0 = +\infty$. This result is due to Shu [19], where it was formulated with total variations. For explicit methods with $k \geqslant 2$, Lenferink [14] showed that

$$K_{\mathrm{LM}} \leqslant \frac{k-p}{k-1}. \tag{9}$$

Hence $K_{\mathrm{LM}} > 0$ is not possible for any method with $p = k$.

The optimal schemes of order 2 are given by [14,19]

$$a_1 = \frac{k(k-2)}{(k-1)^2}, \quad a_k = \frac{1}{(k-1)^2}, \quad b_1 = \frac{k}{k-1}, \tag{10}$$

with the other coefficients zero. Higher-order schemes have been constructed in [14,19], mainly numerically. Our preferred technique is based on a recent approach of [18] for optimizing SSPRK methods. Since we shall use this technique below for deriving new schemes, we describe it here in some detail.

We begin by noting that optimal k-step schemes of order p can be derived by maximizing K_{LM}. Here, the order conditions give $p+1$ relations for the coefficients a_j, b_j [5,11]. However, this formulation of the non-linear programming (NLP) problem does not lend itself easily to numerical solution; see [21] for further discussion. By introducing a dummy variable z, the non-linear programming problem can be reformulated as finding

$$\max_{(a_j,b_j)} z \tag{11a}$$

subject to the $p+1$ order conditions and

$$a_i, b_i \geqslant 0, \quad i = 1, 2, \ldots, k, \tag{11b}$$

$$a_i - z b_i \geqslant 0, \quad i = 1, 2, \ldots, k. \tag{11c}$$

This NLP formulation is comprised of factorable objective and constraint functions and thus is suitable for optimization in BARON [2], which is a commercially-available, deterministic global branch-and-bound optimization program.

To guarantee optimality in BARON we typically need to supply bounds to all the variables. Fortunately we know that all the a_i are bounded by 1 (because $\sum_i a_i = 1$) and all the b_i are bounded by the inverse of K_{LM}. Finding globally optimal schemes and guaranteeing their optimality is surprisingly efficient. For example, BARON5.0 finds the optimal fifty-step, fourth-order scheme and guarantees its optimality in just 0.58 s on a 1.2 GHz Athlon machine.

A list of guaranteed globally optimal schemes for k up to 6 with order p equal to 3 or 4 is given in Table 9 at the end of this paper. Because schemes of this type have most recently been referred to as *strong-stability-preserving* (cf. [3]) and because the coefficients are all non-negative, we denote the optimal k-step, order p linear multistep scheme as $\mathrm{SSPMS}_+(k,p)$.

Fifth- and sixth-order multistep schemes of this type require at least seven steps and do not appear in the table. In view of (9), all methods in the table have $k > p$.

The optimal third-order $\mathrm{SSPMS}_+(4,3)$, $\mathrm{SSPMS}_+(5,3)$ [19,14] and $\mathrm{SSPMS}_+(6,3)$ [14] schemes have been known for some time and we reproduce them here for convenience. The remaining $\mathrm{SSPMS}_+(5,4)$ and $\mathrm{SSPMS}_+(6,4)$ schemes have K_{LM} values that agree with the bounds provided in [14].

2.2. Schemes with spatial downwinding

As noted in [19], the assumption $b_j \geqslant 0$ can be avoided for discretizations of conservation laws (7). If $b_j < 0$, then $F(w_{n-j})$ in (4) should be replaced by $\tilde{F}(w_{n-j})$, where $w' = -\tilde{F}(w)$ is the semi-discretization of the equation with reversed time $u_t - f(u)_x = 0$. Its realization in practice is simply a reversal of the upwind direction in the spatial discretization. Instead of (8) this modification will give the step size restriction

$$\Delta t \leqslant \tilde{K}_{\mathrm{LM}} \Delta t_{\mathrm{FE}}, \qquad \tilde{K}_{\mathrm{LM}} = \min_{1 \leqslant j \leqslant k} \frac{a_j}{|b_j|} \quad \text{if } a_j \geqslant 0 \text{ for all } j, \tag{12}$$

to achieve (5).

The following result gives an upper bound for this threshold factor for second-order schemes. The proof is given in Appendix B.

Theorem 2.1. *For second-order k-step methods we have* $\tilde{K}_{\mathrm{LM}} \leqslant (k-1)/k$. *This upper bound is achieved for* $k \geqslant 2$ *by the schemes (4) with*

$$a_1 = \frac{k^2}{k^2+1}, \quad a_k = \frac{1}{k^2+1}, \quad b_1 = \frac{k^3}{(k-1)(k^2+1)}, \quad b_k = -\frac{k}{(k-1)(k^2+1)},$$

and all other coefficients equal to zero.

Higher-order schemes have been constructed numerically in [19]. We derive globally optimal schemes with downwinding by extending our optimizations for non-negative coefficient schemes.

Following [18], we introduce a dummy variable z and we write $b_i = \sigma_i \tilde{b}_i$ with $\tilde{b}_i = |b_i|$ and $\sigma_i = \mathrm{sgn}(b_i) = \pm 1$. Then the optimization becomes

$$\max_{(a_j, \tilde{b}_j, \sigma_j)} z \tag{13a}$$

subject to the $p+1$ order conditions and the constraints

$$a_i, \tilde{b}_i \geqslant 0, \quad i = 1, 2, \ldots, k, \tag{13b}$$

$$a_i - z\tilde{b}_i \geqslant 0, \quad i = 1, 2, \ldots, k. \tag{13c}$$

Notice that this mixed integer non-linear programming formulation is comprised of factorable objective and constraint functions and that the variables are easily bounded. Thus this is a suitable mathematical formulation for finding guaranteed optimal solutions in BARON. This model may be efficiently treated by solving 2^k NLP problems, each corresponding to one of the possible sign combinations. This leads to a total of 2^k cases each of which only requires a fraction of a second to solve in BARON5.0. Alternatively, the optimization can be carried out in about the same overall CPU time and less programming effort if *product disaggregation* (or distributing products over their sums) is applied to the order conditions. See [22] for details on this technique.

Using the BARON software package, a list of guaranteed globally optimal schemes was constructed for orders $p = 3, 4, 5, 6$ and $k \leqslant 6$. This is presented in Table 10 at the end of this paper. Following the convention described in the previous section, we denote the optimal k-step, order-p scheme with $a_j \geqslant 0$ and unrestricted coefficients b_j as SSPMS$_{\pm}(k,p)$.

The schemes SSPMS$_{\pm}(4,3)$, SSPMS$_{\pm}(5,3)$, SSPMS$_{\pm}(5,4)$, and SSPMS$_{\pm}(6,6)$ are new. Our study for the optimal six-step, third-order scheme is also new; however, there the non-negative coefficient scheme SSPMS$_{+}(6,3)$, first presented in [14], is optimal. The optimal schemes SSPMS$_{\pm}(3,3)$, SSPMS$_{\pm}(4,4)$ presented in Table 10 essentially agree with earlier schemes from Gottlieb et al. [3]. Some improvements were found in the remaining three cases over earlier studies [19,3]. Specifically, 16%, 12% and 1% improvements in $\tilde{K}_{\mathrm{LM}}$ were found for SSPMS$_{\pm}(6,4)$, SSPMS$_{\pm}(5,5)$, and SSPMS$_{\pm}(6,5)$, respectively.

Comparing the SSPMS$_{\pm}(k,p)$ and the SSPMS$_{+}(k,p)$ schemes, it should be noted that for the SSPMS$_{\pm}(k,p)$ schemes both function evaluations F_n and $\tilde{F}_n$ will be needed. If more than one processor is available, these evaluations can be carried out in parallel. On a serial machine, however, these schemes will be approximately two times more expensive per step. Moreover, the use of downwind discretizations may add some numerical diffusion that will persist even for small step sizes; see the test results in Section 4.

3. Boundedness for higher-order methods

The above monotone multistep schemes are not competitive with the Runge–Kutta schemes of [10,16,21]. However, by considering the multistep schemes in combination with starting procedures, it is possible to consider schemes that satisfy the boundedness property (6) with a constant M whose size is determined by the starting procedure [7].

This section contains derivations of optimal boundedness results for explicit linear multistep methods of order $p = 3, 4, 5, 6$. To study the boundedness property (6), with $M \geqslant 1$, it is not necessary to specify the starting schemes: while the value of M may vary according to the starting procedure, the boundedness property itself is independent of the chosen startup. (We remark that this result uses the fact that the startup is only applied for a fixed number of times. See [6] for the proof.)

3.1. Reformulations

The derivation of boundedness results is largely based on suitable reformulations of the schemes, whereby a k-step scheme is first rewritten as an equivalent $(k+1)$-step scheme with a free parameter, then as a $(k+2)$-step scheme with two free parameters, etc., up to the starting values. The free parameters can then be selected such that the scheme has non-negative coefficients.

To keep the presentation concise and clear, we give such a reformulation here in detail only for three-step schemes; the general formulas can be found in [6]. Consider (4) with $k = 3$. Then by subtracting and adding $\theta_1 \cdots \theta_j w_{n-j}$, $j = 1, 2, \ldots, n-3$, substituting w_{n-j} in terms of w_{n-j-i}, $i = 1, 2, 3$, and collecting terms, it follows that w_n can be expressed as

$$w_n = \sum_{j=1}^{n-3} (\alpha_j w_{n-j} + \beta_j \Delta t F_{n-j}) + \sum_{i=0}^{2} \left(\alpha^R_{n,n-i} w_i + \beta^R_{n,n-i} \Delta t F_i \right), \tag{14}$$

where the coefficients α_j, β_j are given by

$$\begin{aligned}
&\alpha_1 = a_1 - \theta_1, \quad \alpha_2 = a_2 + a_1\theta_1 - \theta_1\theta_2, \quad \alpha_3 = a_3 + a_2\theta_1 + a_1\theta_1\theta_2 - \theta_1\theta_2\theta_3,\\
&\alpha_j = \left(\prod_{k=1}^{j-3} \theta_k \right) (a_3 + a_2\theta_{j-2} + a_1\theta_{j-2}\theta_{j-1} - \theta_{j-2}\theta_{j-1}\theta_j), \quad j \geqslant 4,\\
&\beta_1 = b_1, \quad \beta_2 = b_2 + b_1\theta_1, \quad \beta_3 = b_3 + b_2\theta_1 + b_1\theta_1\theta_2,\\
&\beta_j = \left(\prod_{k=1}^{j-3} \theta_k \right) (b_3 + b_2\theta_{j-2} + b_1\theta_{j-2}\theta_{j-1}), \quad j \geqslant 4
\end{aligned}$$

and the coefficients of the remainder term are

$$\alpha^R_{n,n-i} = \sum_{j=3-i}^{3} a_j \left(\prod_{k=1}^{n-i-j} \theta_k \right), \quad \beta^R_{n,n-i} = \sum_{j=3-i}^{3} b_j \left(\prod_{k=1}^{n-i-j} \theta_k \right), \quad 0 \leqslant i \leqslant 2.$$

For k-step methods with $k \geqslant 4$ we can proceed similarly. In the above reformulation (14) we get the same expressions for $\alpha_1, \alpha_2, \alpha_3$ and $\beta_1, \beta_2, \beta_3$; the other α_j, β_j will then involve more terms.

We shall take $\theta_i \geqslant 0$ such that

$$\alpha_j \geqslant 0, \quad \beta_j \geqslant 0 \quad \text{for all } j \geqslant 1, \tag{15}$$

and we define

$$C_{\mathrm{LM}} = \max_{\{\theta_i\}_{i \geqslant 1}} \min_{j \geqslant 1} \frac{\alpha_j}{\beta_j}. \tag{16}$$

In the search for favorable schemes we will require that

$$\theta_j = \theta_* < 1 \quad \text{for all } j \geqslant j_*, \tag{17}$$

since any zero-stable, irreducible scheme with $C_{\mathrm{LM}} > 0$ must have this property [6]. Under these assumptions it follows that the boundedness property (6) holds with $M \geqslant 1$ for step sizes

$$\Delta t \leqslant C_{\mathrm{LM}} \Delta t_{\mathrm{FE}}. \tag{18}$$

To obtain results for genuine monotonicity, that is, $M = 1$, it is also necessary to study the coefficients $\alpha^R_{n,n-i}$ and $\beta^R_{n,n-i}$ of the remainder term in (14) and to include specific starting procedures. For a detailed analysis, we refer to [7] for the case $k = 2$ and to [6] for $k \geqslant 3$.

3.2. Optimizations of C_{LM}

Two-step, second-order explicit methods can be studied by hand, as it was done in [7]. Methods involving more steps are more involved, and naturally lead us to consider numerical optimization techniques. Following Section 2.1, we formulate the optimization problem by introducing a dummy variable z that corresponds to C_{LM}; however, now all the α_i, β_i must be constrained to be non-negative. We have carried out extensive optimizations in BARON to determine numerically optimal schemes. A guarantee of optimality is not sought since the overall complexity of the optimization problem makes this much more difficult.

By increasing the number of θ values, we hope to obtain schemes with improved time-stepping restrictions. However, some bound on the number of θ values must be imposed to make the optimization practical. In our derivations, values of j_* ranging from 15 to 25 were used, depending on the order of the method under consideration (higher-order methods required more θ values to obtain large CFL coefficients). Further increases in j_* were not found to substantially increase C_{LM} (see Appendix A of [6] for precise details) and produced no discernable improvement in numerical tests. Indeed, for $(k,p) = (3,3)$ and $(k,p) = (5,5)$ the j_* values were chosen to be large enough that further increases produced no improvement whatsoever in C_{LM}.

The schemes that are found this way for given step number k and order p will be denoted as TVB(k,p). Somewhat surprisingly, seeking optimal schemes often led to a value $\theta_* = 0$. This means that all coefficients α_j, β_j are zero for $j \geqslant k + j_*$, and hence the reformulation then gives a l-step scheme, $l = k + j_* - 1$, with non-negative coefficients. Using [19], it is easily seen that this extended scheme is monotone for arbitrary starting values (i.e., it satisfies monotonicity property (5) for arbitrary staring values) provided $\Delta t \leqslant C_{\mathrm{LM}} \Delta t_{\mathrm{FE}}$ [6]. Clearly it is also reducible to the original k-step method [5], so the extension should primarily be regarded for theoretical interest. Schemes with $\theta_* = 0$ will be denoted by TVB$_0(k,p)$.

Finally we note that for all the new schemes presented in this section the error constants turned out to be of moderate size. These error constants C, properly defined in [5, p. 373], provide a good measure for the leading term $C\Delta t^p$ in the global error.

3.3. An order-3 scheme

We first optimize C_{LM} over the class of three-step, third-order linear multistep schemes with 15 θ values. This yields a scheme that satisfies the boundedness property (6) with $M \geqslant 1$ provided $\Delta t \leqslant 0.537 \Delta t_{\mathrm{FE}}$. The coefficients are given in Table 1. It is noteworthy that the optimization leads to $\theta_{10} = 0$, implying this scheme can be rewritten as a 12-step scheme that is monotone with arbitrary starting values. Because of this property, we will refer to this scheme as TVB$_0(3,3)$.

It is interesting to compare this TVB$_0(3,3)$ scheme against the third-order extrapolated BDF scheme (eBDF3)

Table 1
The coefficients of the numerically optimal three-step, third-order linear multistep scheme

$TVB_0(3,3)$	a_i	b_i	C_{LM}
$i = 1$	1.908535476882378	1.502575553858997	0.537252303224424
$i = 2$	−1.334951446162515	−1.654746338401493	
$i = 3$	0.426415969280137	0.670051276940255	

$$w_n = \frac{18}{11}w_{n-1} - \frac{9}{11}w_{n-2} + \frac{2}{11}w_{n-3} + \frac{18}{11}\Delta t F_{n-1} - \frac{18}{11}\Delta t F_{n-2} + \frac{6}{11}\Delta t F_{n-3}, \tag{19}$$

which is the best reported third-order scheme in [7]. Because its threshold value is given by $C_{LM} = 7/18$, the new scheme $TVB_0(3,3)$ gives a 38% improvement over eBDF3 in allowable (stable) step size, for which (6) is ensured.

The new $TVB_0(3,3)$ scheme also has a relatively large linear stability region, showing where linear stability is valid for the scalar, complex test equation $w' = \lambda w$, $z = \Delta t\lambda$. The $TVB_0(3,3)$ stability region includes a part of the imaginary axis. See Fig. 1 for a comparison of the stability region of this scheme and the eBDF3 scheme.

Although the form of the stability regions is not directly related to monotonicity properties, it seems that for higher-order spatial discretizations violation of the linear (von Neumann) stability conditions often leads to inaccurate solutions due to numerical *compression* of smooth solutions; see for instance [8, Section 1.3] for an illustration. Having a portion of the imaginary axis and some region to the left of it in the stability region ensures that the scheme will be stable under appropriate CFL restriction in the classical, linear sense for any spatial discretization.

3.4. Fourth-order schemes

3.4.1. Four-step schemes

We direct our attention next to the class of four-step, fourth-order linear multistep methods. In the reformulations for this class, we were unable to find schemes which allowed arbitrary starting values in an extended version (i.e., $\theta_* = 0$). Moreover, taking $\theta_j = \theta_*$ for all $j \geqslant j_*$ we found that C_{LM} increases as $\theta_* \in [0,1)$ increases. Unfortunately the choice $\theta_* = 1$ does not lead to a scheme that is stable; the scheme turned out to have two characteristic roots equal to one, giving weak instability. For θ_* close

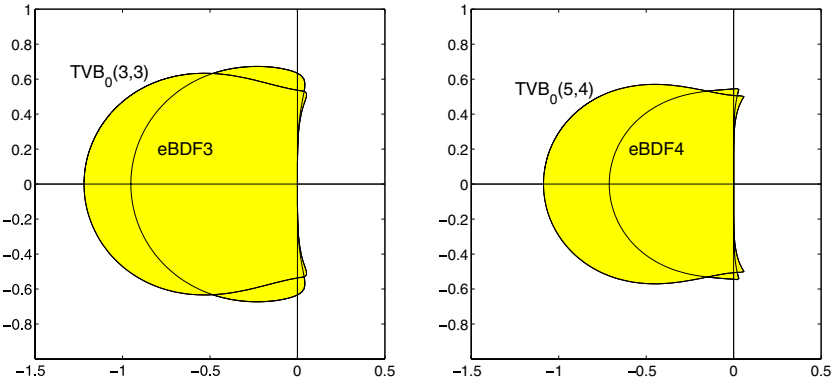

Fig. 1. Stability regions for the eBDF3 and $TVB_0(3,3)$ schemes (left plot) and the eBDF4 and $TVB_0(5,4)$ schemes (right plot). The TVB(4,4) region is not shown since it closely agrees with the $TVB_0(5,4)$ region.

to 1, the (scaled) error constants [5, p. 373] are large. Selecting an appropriate scheme is therefore quite interesting and subtle, since larger θ_* values give larger C_{LM} values while smaller θ_* values give better accuracy and also seem to minimize the possibility of oscillations arising from the startup procedures when $M > 1$.

On the balance, we bias our choice towards large time steps by taking $\theta_* = 0.7$ giving a restriction of $\Delta t \leqslant 0.458\Delta t_{\mathrm{FE}}$. This is approximately 15% less than the limiting case $\theta_* = 1$ ($C_{\mathrm{LM}} = 0.537$ for $\theta_* = 1$). We provide the scheme to 15 decimal digits in Table 2 and remark that the $\theta_{15} = 0.7$ constraint was active for this scheme.

It is natural to compare this TVB(4,4) scheme against the fourth-order extrapolated BDF scheme (eBDF4)

$$w_n = \frac{48}{25}w_{n-1} - \frac{36}{25}w_{n-2} + \frac{16}{25}w_{n-3} - \frac{3}{25}w_{n-4} + \frac{48}{25}\Delta t F_{n-1} - \frac{72}{25}\Delta t F_{n-2} + \frac{48}{25}\Delta t F_{n-3} - \frac{12}{25}\Delta t F_{n-4}. \tag{20}$$

Since the non-linear time-stepping restriction of eBDF4 is given by $C_{\mathrm{LM}} = 7/32$, the new scheme provides for a 109% improvement in allowable (stable) step size over the best reported scheme (eBDF4) in [7]. Once again, the stability region of new scheme includes part of the imaginary axis and it compares favorably against that of the eBDF4 scheme; cf. Fig. 1.

3.4.2. Five-step schemes

If we consider five-step schemes, then it is possible to find fourth-order schemes that can be rewritten in an extended form that allows arbitrary starting values. For example, optimizing C_{LM} over the class of five-step, fourth-order linear multistep schemes with 15 non-zero θ values yields the $\mathrm{TVB}_0(5,4)$ scheme presented in Table 3. This scheme satisfies the boundedness property (6) with $M \geqslant 1$ provided $\Delta t \leqslant 0.45\Delta t_{\mathrm{FE}}$. Since $\theta_{16} = 0$, this scheme can be rewritten as a 20-step scheme with non-negative coefficients. The stability region of $\mathrm{TVB}_0(5,4)$ includes part of the imaginary axis and essentially coincides with TVB(4,4). See Fig. 1.

By increasing the number of non-zero θ values, we can obtain slightly larger C_{LM} values. For example, optimizations using 30 θ values produced a scheme with $C_{\mathrm{LM}} = 0.471$. We do not reproduce that scheme here as it had similar behavior in numerical tests to $\mathrm{TVB}_0(5,4)$.

Table 2
The coefficients of the numerically optimal four-step, fourth-order linear multistep scheme

TVB(4,4)	a_i	b_i	C_{LM}
$i = 1$	2.628241000683208	1.618795874276609	0.458583744721242
$i = 2$	−2.777506277494861	−3.052866947601049	
$i = 3$	1.494730011212510	2.229909318681302	
$i = 4$	−0.345464734400857	−0.620278703629274	

Table 3
The coefficients of the numerically optimal five-step, fourth-order linear multistep scheme

$\mathrm{TVB}_0(5,4)$	a_i	b_i	C_{LM}
$i = 1$	3.089334754787739	1.629978886421390	0.450202335599730
$i = 2$	−3.997727108450201	−3.839438825282836	
$i = 3$	2.799704082644115	3.698752623531085	
$i = 4$	−1.069321620028803	−1.688757722449064	
$i = 5$	0.178009891047150	0.305220798719644	

3.5. An order-5 scheme

We next study five-step, fifth-order linear multistep methods. For optimizing C_{LM} over this class we used twenty-five θ values. This yields a scheme with $M \geqslant 1$ provided $\Delta t \leqslant 0.377\Delta t_{\mathrm{FE}}$. The coefficients of this optimal scheme are given in Table 4. This scheme has $\theta_{21} = 0$ which implies that it can be rewritten as a 25 step scheme that is monotone with arbitrary starting values.

As a basis for comparison, we consider the fifth-order extrapolated BDF scheme (eBDF5), which is given by

$$w_n = \frac{300}{137}w_{n-1} - \frac{300}{137}w_{n-2} + \frac{200}{137}w_{n-3} - \frac{75}{137}w_{n-4} + \frac{12}{137}w_{n-5} + \frac{300}{137}\Delta tF_{n-1} - \frac{600}{137}\Delta tF_{n-2} + \frac{600}{137}\Delta tF_{n-3} - \frac{300}{137}\Delta tF_{n-4} + \frac{60}{137}\Delta tF_{n-5}. \tag{21}$$

The non-linear time-stepping restriction of eBDF5 is $\Delta t \leqslant 0.0867\Delta t_{\mathrm{FE}}$ so $\mathrm{TVB}_0(5,5)$ gives a 335% improvement in allowable (stable) step size over this extrapolated BDF scheme. The linear stability of the scheme is also favorable when compared against eBDF5; see Fig. 2. However, we know the scheme cannot include the imaginary axis near the origin since it is impossible for any five-step, fifth-order scheme to do so [9]. On the other hand, it is seen that the boundary of the stability region stays very close to a segment of the imaginary axis and the corresponding maximal amplification factors on the imaginary axis are very close to 1. Because optimizations using $k = 6, 7$ gave similar time-stepping restrictions (the C_{LM} values were 0.379 and 0.395, respectively) and did not produce a stricter linear stability near the origin we focus our attention on the five-step scheme, $\mathrm{TVB}_0(5,5)$.

Table 4
The coefficients of the numerically optimal five-step, fifth-order linear multistep scheme

$\mathrm{TVB}_0(5,5)$	a_i	b_i	C_{LM}
$i = 1$	3.308891758551210	1.747442076919292	0.377052834833475
$i = 2$	−4.653490937946655	−4.630745565661800	
$i = 3$	3.571762873789854	5.086056171401077	
$i = 4$	−1.504199914126327	−2.691494591660196	
$i = 5$	0.277036219731918	0.574321855183372	

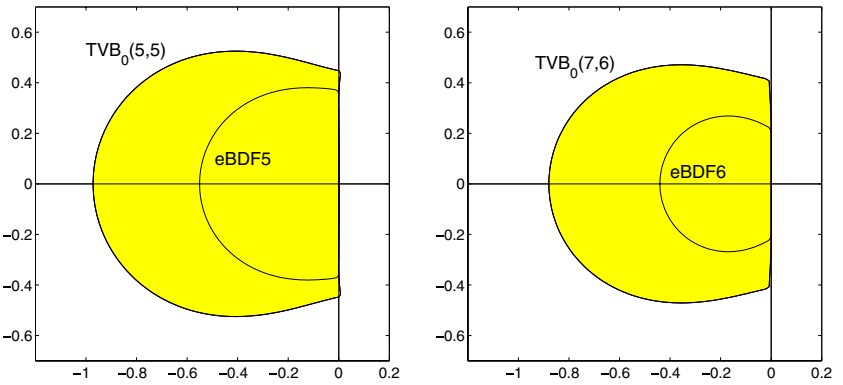

Fig. 2. Stability regions for the eBDF5 and $\mathrm{TVB}_0(5,5)$ schemes (left plot) and the eBDF6 and $\mathrm{TVB}_0(7,6)$ schemes (right plot). The TVB(6,6) region is not plotted since it closely agrees with the $\mathrm{TVB}_0(7,6)$ region.

3.6. Sixth-order schemes

3.6.1. Six-step schemes

The results for the sixth-order extrapolated BDF method (eBDF6) are less favorable than for lower-order eBDF schemes.

Theorem 3.1. *For the eBDF6 scheme no positive C_{LM} value in (16) exists.*

Proof. To show that we cannot have $C_{\mathrm{LM}} > 0$, note that the first step of the reformulation (14) for eBDF6 will give

$$w_n = \left(\frac{360}{147} - \theta\right) w_{n-1} + \frac{360}{147}\Delta t F_{n-1} + \left(\frac{360}{147}\theta - \frac{15}{2}\right) w_{n-2} + \left(\frac{360}{147}\theta - \frac{720}{147}\right)\Delta t F_{n-2} + \cdots$$

with $\theta = \theta_1$. It is impossible for both $(\frac{360}{147} - \theta)$ and $(\frac{360}{147}\theta - \frac{720}{147})$ to be positive; hence the scheme does not possess a positive threshold value C_{LM}. □

Rewriting the general class of six-step methods of order 6 using additional steps, we were unable to find extended schemes that allow for monotonicity with arbitrary starting values. Taking 25 distinct θ values and $\theta_j = \theta_*$ for all $j \geqslant j_* = 25$ we found that C_{LM} increases as $\theta_* \in [0, 1)$ increases. Based on a variety of numerical tests, it was found that the choice $\theta_* = 0.75$ gives a relatively large $C_{\mathrm{LM}} = 0.328$ and moderate error constant, while adequately minimizing the possibility of oscillations arising from the startup procedures. See Table 5 for the coefficients of this scheme and Fig. 2 for the linear stability region. Similar to the fifth-order case, the stability region of the TVB(6, 6) scheme does not contain a segment of the imaginary axis near the origin, but its boundary is for a large part very close to the imaginary axis.

3.6.2. Seven-step schemes

If we consider seven-step schemes, then it is possible to find schemes of order 6 that can be rewritten as a scheme with larger step number and non-negative coefficients, giving monotonicity for arbitrary starting values.

Optimization of C_{LM} over the class of seven-step, sixth-order linear multistep schemes with 25 non-zero θ values yields the $\mathrm{TVB}_0(7, 6)$ scheme presented in Table 6. This scheme satisfies the boundedness property (6) with $M \geqslant 1$ provided $\Delta t \leqslant 0.309\Delta t_{\mathrm{FE}}$. Since $\theta_{26} = 0$, this scheme can be rewritten as an 32-step scheme with non-negative coefficients. The stability region of $\mathrm{TVB}_0(7, 6)$ essentially coincides with TVB(6, 6) and does not contain a segment of the imaginary axis near the origin. The stability region is displayed in Fig. 2.

Table 5
The coefficients of the numerically optimal six-step, sixth-order linear multistep scheme

TVB(6, 6)	a_i	b_i	C_{LM}
$i = 1$	4.113382628475685	1.825457674048542	0.328491643359885
$i = 2$	−7.345730559324184	−6.414174588309508	
$i = 3$	7.393648314992094	9.591671249204753	
$i = 4$	−4.455158576186636	−7.583521888026967	
$i = 5$	1.523638279938299	3.147082225022105	
$i = 6$	−0.229780087895259	−0.544771649561925	

Table 6
The coefficients of the numerically optimal seven-step, sixth-order linear multistep scheme

$TVB_0(7,6)$	a_i	b_i	C_{LM}
$i = 1$	4.611532883607545	1.861015137800509	0.309253747416378
$i = 2$	−9.451321766751356	−7.511070082780818	
$i = 3$	11.294453144657830	13.266237470507250	
$i = 4$	−8.568419982721693	−13.059962115416270	
$i = 5$	4.138363606421970	7.520216192319446	
$i = 6$	−1.174917528050790	−2.389309837695513	
$i = 7$	0.150309642836489	0.325922452117498	

4. Numerical illustrations

In this section, we examine the numerical behavior of our new linear multistep methods and compare with more classical monotonicity-preserving schemes, mentioned in Section 2, and some optimal SSPRK schemes, denoted as SSPRK(s,p) where s is the number of stages and p the order. Our focus here is to illustrate the monotonicity and stability behavior of the schemes rather than to provide a detailed accuracy study. If a study of the temporal accuracy was desired it would be more appropriate to consider systems with smooth solutions where the spatial discretization errors are dominated by the time stepping errors.

4.1. Linear monotonicity test

As a first, simple test we consider the maximum principle for the linear advection problem

$$u_t + u_x = 0$$

on spatial interval $0 \leqslant x \leqslant 1$, with inflow boundary condition $u(0,t) = 0$ and initial step function $u(x,0) = 1$ on $(0, 1/2]$ and 0 elsewhere. The semi-discrete system in $\mathbb{R}^m$ is obtained by first-order upwind discretization in space with constant mesh width $\Delta x = 1/m$. For the test $m = 100$ is taken.

The PDE solution satisfies the maximum principle $0 \leqslant u(x,t) \leqslant 1$ and the same holds for the semi-discrete system. This property will be examined for the fully discrete solutions. The maximum principle

Table 7
Linear monotonicity test: maximal Courant numbers for the optimal k-step methods, $k = 3,4$

	eBDF3	$SSPMS_+(3,2)$	$TVB_0(3,3)$	eBDF4	$SSPMS_+(4,3)$	TVB(4,4)
C_{LM}	0.39	0.50	0.53	0.22	0.33	0.45
Exper.(FE)	0.41	0.50	0.53	0.26	0.34	$0.46^{(*)}$
Exper.(RK4)	0.43	0.50	0.53	0.30	0.35	$0.51^{(*)}$

The results for TVB(4,4) were obtained with $\epsilon = 10^{-12}$; this is indicated by the entries$^{(*)}$.

Table 8
Linear monotonicity test: maximal Courant numbers for the optimal k-step methods, $k = 5,6,7$

	eBDF5	$TVB_0(5,5)$	$TVB_0(5,4)$	eBDF6	TVB(6,6)	$TVB_0(7,6)$
C_{LM}	0.08	0.37	0.45	0.00	0.32	0.30
Exper.(FE)	0.17	0.37	0.47	–	0.32	0.32
Exper.(RK4)	0.21	0.38	0.50	–	0.37	0.34

could be replaced equivalently by max-norm monotonicity by considering an equivalent advection problem with $v(x,t) = 2u(x,t) - 1$.

Starting values for the multistep schemes were computed by the forward Euler method (FE) and the classical fourth-order Runge–Kutta method (RK4). Note that for this simple linear problem the classical Runge–Kutta method is monotone. For actual applications, a natural choice would be to use a monotone starting scheme of order $p-1$ or p for a multistep scheme of order p, in combination with a suitable spatial discretization. For this monotonicity test, using the first-order upwind discretization, only the choices FE and RK4 were considered for convenience.

Subsequently, the largest Courant numbers $\Delta t/\Delta x \in \{0.01, 0.02, \ldots\}$ were determined such that

$$-\epsilon \leqslant w_n \leqslant 1+\epsilon \quad \text{for } n = 1, 2, \ldots, 1000,$$

with inequalities for the vectors $w_n \in \mathbb{R}^m$ componentwise. Of course, if $\epsilon = 0$ this is a genuine maximum principle. In exact arithmetic we could take $\epsilon = 0$ for a monotone scheme with rational coefficients. To cater for round-off and the fact that our schemes are not genuinely monotone we took as standard value $\epsilon = 10^{-15}$. However, for the TVB(4,4) scheme ϵ values larger than this default value were needed; those results were obtained with $\epsilon = 10^{-12}$. In Tables 7 and 8 the maximal Courant numbers are listed for the most interesting optimal schemes. For comparison, also the entries for the eBDF-schemes are presented.

4.2. Non-linear test: Burgers' equation

To further investigate the behavior of our time-stepping schemes, we consider one of Laney's five test problems [12], the evolution of a square wave by Burgers' equation

$$\frac{\partial u}{\partial t} + \frac{\partial}{\partial x}\left(\frac{1}{2}u^2\right) = 0$$

on the spatial interval $-1 \leqslant x \leqslant 1$ with periodic boundary conditions. In this test case, the discontinuous initial conditions

$$u(x,0) = \begin{cases} 1 & \text{for } |x| < 1/3, \\ -1 & \text{for } 1/3 < |x| \leqslant 1, \end{cases}$$

are evolved to time $t = 0.3$ using a constant grid spacing of $\Delta x = 1/320$. In this example, the jump at $x = 1/3$ remains a steady shock and the jump at $x = -1/3$ creates a simple centered expansion fan between $c_1 = -1/3 - t$ and $c_2 = -1/3 + t$. Until the shock and expansion fan intersect, at time $t = 2/3$, the exact solution is [12]

$$u(x,t) = \begin{cases} -1 + 2\frac{x-c_1}{c_2-c_1} & \text{for } c_1 < x < c_2, \\ 1 & \text{for } c_2 < x < 1/3, \\ -1 & \text{elsewhere.} \end{cases}$$

The example is particularly interesting because it illustrates the behaviors near sonic points ($u = 0$) that correspond to an expansion fan and a compressive shock.

Similar to [21,16], we choose the finite-difference Shu-Osher schemes (ENO-type) for spatial discretization of the equation. These discretizations are derived using flux reconstruction and have a variety of desirable properties. For example, they naturally extend to an arbitrary order of accuracy in space, and they are independent of the time discretization, thus allowing experimentation with different time discretization methods. Moreover, educational codes are also freely available [12,13], an attribute which is desirable for standardizing numerical studies. In our simulations we take the spatial order of accuracy in Δx to be

the same as the temporal order of accuracy p. Flux splitting is taken as in [21,16]. For further details on the underlying discretization as well as a code for the spatial discretization, see [12,13].

4.2.1. Third-order experiments

To quantify the accuracy of the computed solution, we use the logarithm of the discrete L_1 errors at time $t_n = 0.3$,

$$\log_{10}\left(\frac{1}{m}\sum_{i=1}^{m}|w_i^n - u(x_i, t_n)|\right),$$

where m is the number of grid points and w_i^n is the fully discrete solution in grid point x_i at time t_n. A plot of the error for a selection of third-order methods is given in Fig. 3. To ensure a fair comparison for methods with a different number of function evaluations, the error is plotted as a function of the *effective CFL number*, $\Delta t/(s\Delta x)$ for a method taking s function evaluations per step, rather than the CFL number itself. This implies that for a particular plot, the total number of function evaluations at a particular abscissa value will be the same for each scheme. We started the computations with an effective CFL number of 0.02 and continued until the numerical scheme produced overflow (complete instability).

In this test example, we compare a number of three-step, third-order linear multistep schemes and the optimal three-stage, third-order SSP Runge–Kutta method SSPRK(3, 3) that was derived by Shu and Osher in [20,19] and Kraaijevanger in [10]. All the multistep schemes are started using the SSPRK(3, 3) scheme. Of the schemes considered, the best performance is given by the new $TVB_0(3, 3)$ scheme and the poorest performance is given by the classical SSP multistep scheme $SSPMS_{\pm}(3, 3)$. In particular, the $TVB_0(3, 3)$ scheme allows a 284% increase in the effective time step over $SSPMS_{\pm}(3, 3)$ and 22% increase over the popular SSPRK(3, 3) scheme. The extrapolated BDF scheme also performs well, providing a 15% increase in the effective timestep over SSPRK(3, 3). We remark that $TVB_0(3, 3)$ and eBDF3 each require one function evaluation per timestep while SSPRK(3, 3) requires three and $SSPMS_{\pm}(3, 3)$ requires two (due to its use of a downwind-biased operator).

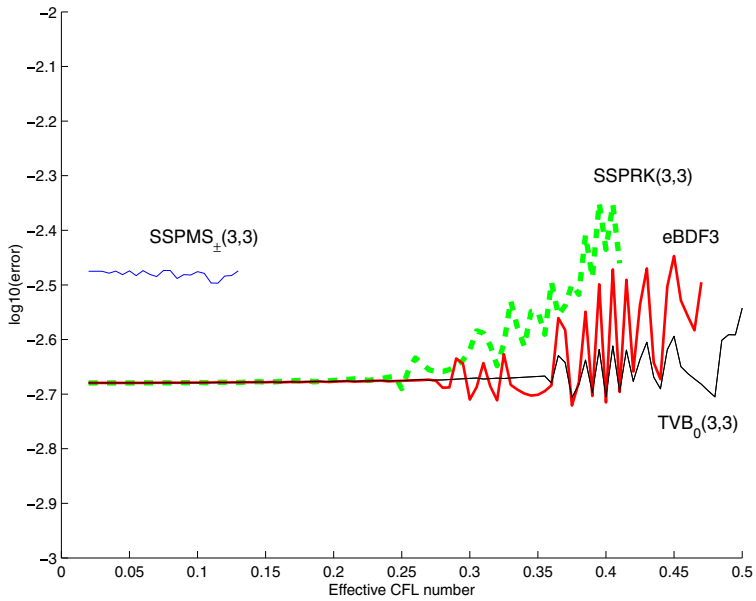

Fig. 3. Burgers' equation: L_1 errors as a function of the effective CFL number for selected third-order schemes.

The oscillations in the error plots suggest that oscillations in the solutions arise for large enough time steps (and before the methods produce overflow). An examination of the total variation (TV) of the solutions verifies this conjecture and also leads us to recommend the new $TVB_0(3,3)$ scheme. In particular, we remark that the TV-increase for $TVB_0(3,3)$ remains *very* small (less than 10^{-12}) up to an effective CFL number of 0.375. This represents an improvement in the time step-size of 213%, 25%, and 23% over the $SSPMS_{\pm}(3,3)$, eBDF3, and SSPRK(3,3) schemes, respectively.

An assessment of the quality of the solution may also be carried out by examining the solution profiles themselves. See Fig. 4 for some zoom-ins near the shock. Plot (b) illustrates that for very small timesteps the $SSPMS_{\pm}(3,3)$ scheme produces more smearing than other schemes. As explained in [16] this can be attributed to its use of downwind-biased spatial discretizations. Plot (c) gives an example with larger timesteps. In this example, the $SSPMS_{\pm}(3,3)$ is no longer stable and SSPRK(3,3) exhibits a clear undershoot. The eBDF3 and $TVB_0(3,3)$ schemes both give a good treatment of the shock, with $TVB_0(3,3)$ being somewhat less dissipative. Larger timesteps (corresponding to an effective CFL number of 0.45) are illustrated in plot (d). In this experiment, SSPRK(3,3) has gone unstable and eBDF3 exhibits oscillations. The $TVB_0(3,3)$ scheme, however, performs well without any visible oscillations or excessive smearing.

Numerical experiments using $SSPMS_{+}(4,3)$ are also possible. Notice, however, that this scheme has a smaller CFL coefficient and requires more steps than eBDF3 or $TVB_0(3,3)$. Furthermore, the scheme

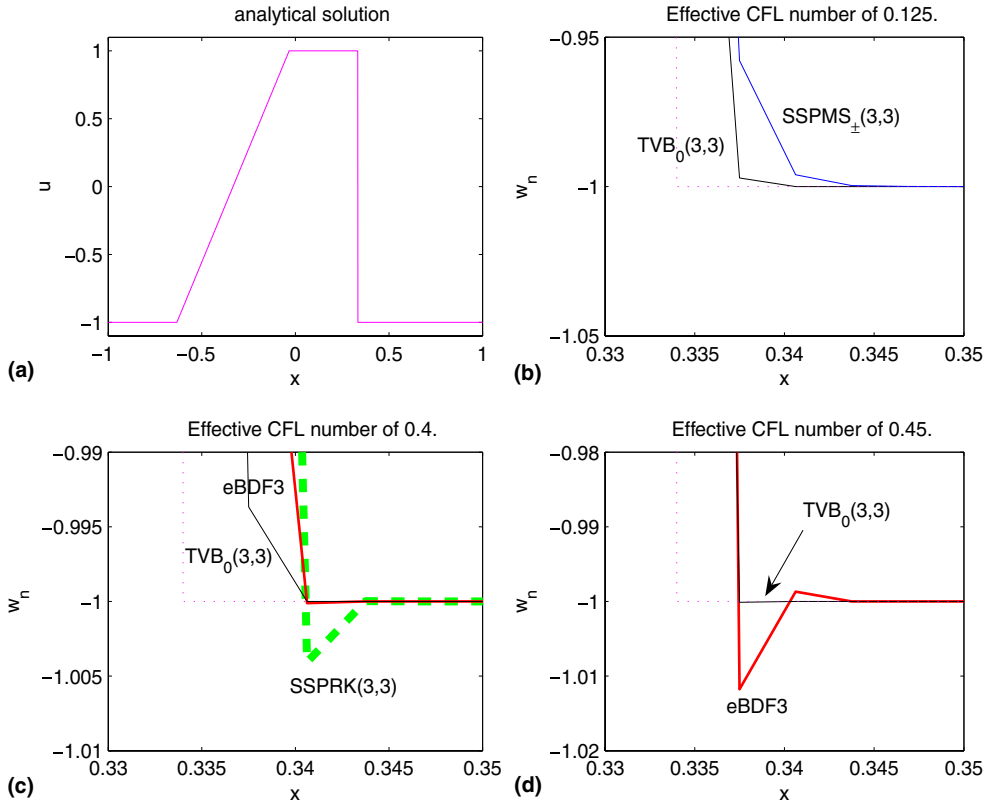

Fig. 4. Plots of the solution for third-order methods applied to the Burgers' equation example. (a) The analytical solution. See also the dotted line in zoom-in plots (b)–(d). (b) Numerical results using an effective CFL number of 0.125. eBDF3 and SSPRK(3,3) closely agree with $TVB_0(3,3)$. (c) Numerical results using an effective CFL number of 0.4. $SSPMS_{\pm}(3,3)$ is unstable. (d) Numerical results using an effective CFL number of 0.45. $SSPMS_{\pm}(3,3)$ and SSPRK(3,3) are unstable.

has no theoretical advantage (in terms of effective CFL coefficient) over the classical one-step SSPRK(3, 3) method even though additional memory is required. Our numerical tests were also unable to uncover a compelling reason to use $SSPMS_+(4,3)$ since it produced oscillations and complete instability for smaller effective CFL numbers than any of SSPRK(3, 3), eBDF3 and $TVB_0(3,3)$.

4.2.2. Fourth-order experiments

For a selection of fourth-order schemes the L_1 errors as a function of the effective CFL number are plotted in Fig. 5. All the multistep schemes are started using the optimal SSPRK(5, 4) scheme [10,21]. We remark that the TVB(4, 4) scheme gave similar results to $TVB_0(5,4)$, so its plot is omitted for clarity. The $SSPMS_+(5,4)$ scheme was also tested, but its plot is not included since its stability is not competitive with $SSPMS_\pm(4,4)$.

Of the schemes considered here, the best performance is given by the new scheme $TVB_0(5,4)$ and the weakest performance is given by the classical SSP multistep scheme $SSPMS_\pm(4,4)$. More specifically, the $TVB_0(5,4)$ scheme allows a 600% increase in the effective time step over $SSPMS_\pm(4,4)$, a 13% increase over the SSPRK(5, 4) scheme, and a 2% increase over TVB(4, 4). The extrapolated BDF scheme is not competitive with either SSPRK(5, 4) or $TVB_0(5,4)$, although its performance is much better than $SSPMS_\pm(4,4)$.

Similar to the third-order case, an examination of the solution profiles for small timesteps indicates that $SSPMS_\pm(4,4)$ is more dissipative than other fourth-order schemes. If we move to a larger timestep (corresponding to an effective CFL number of 0.275) we find that eBDF4 produces an undershoot, while $TVB_0(5,4)$ and SSPRK(5, 4) both perform well. Indeed, $TVB_0(5,4)$ performs well (i.e., without any visible oscillations or excessive smearing) even when eBDF4 and SSPRK(5, 4) are unstable. See Fig. 6 for the corresponding solution profiles.

The SSPRK(5, 4), TVB(4, 4) and $TVB_0(5,4)$ schemes all limit oscillations to modest levels. In particular, we note that the TV-increase for each of these schemes first exceeds 10^{-6} at an effective CFL number of 0.37. On the other hand, the TV-increase for eBDF4 first exceeds 10^{-6} at an effective CFL number of 0.24. In most applications the small, bounded oscillations produced by $TVB_0(5,4)$ and TVB(4, 4) should

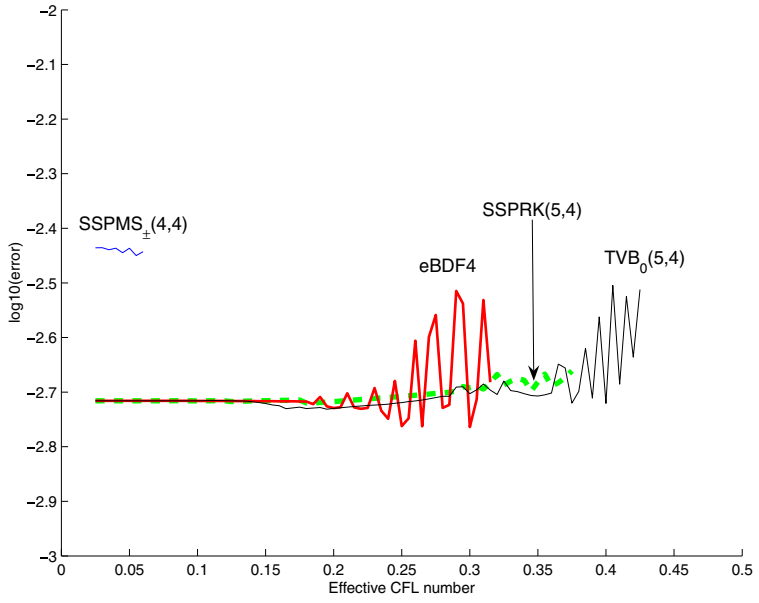

Fig. 5. Burgers' equation: L_1 errors as a function of the effective CFL number for selected fourth-order schemes.

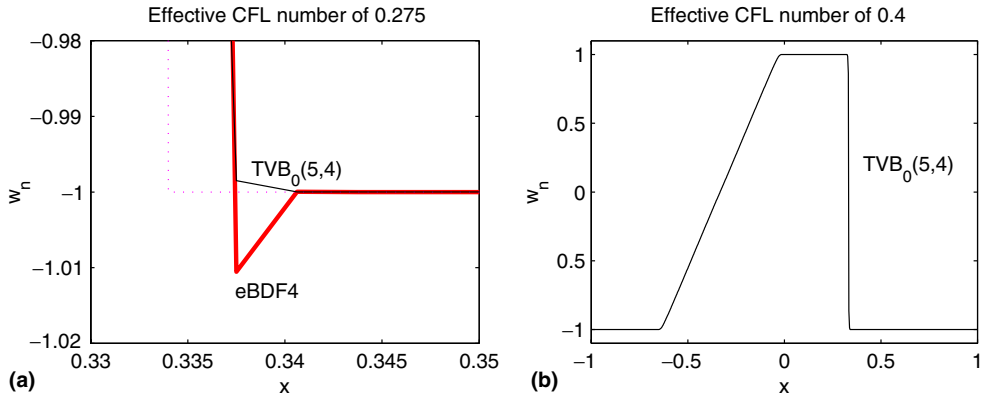

Fig. 6. Plots of the solution for fourth-order methods applied to the Burgers' equation example. (a) Zoom-in of numerical results using an effective CFL number of 0.275. $\text{SSPMS}_{\pm}(4,4)$ is unstable and SSPRK(5,4) closely agrees with $\text{TVB}_0(5,4)$. (b) Global solution using an effective CFL number of 0.4. $\text{SSPMS}_{\pm}(4,4)$, eBDF4 and SSPRK(5,4) are unstable.

be quite acceptable. However, fifth- and higher-order schemes produce larger oscillations. The source of these oscillations receives some attention in the next subsection.

4.2.3. Higher-order experiments

The L_1 errors as a function of the effective CFL number are plotted for a selection of fifth-order schemes in Fig. 7. Our tests include the new $\text{TVB}_0(5,5)$ scheme and the eBDF5 scheme. As a basis for comparison, we also include a recent nine-stage, fifth-order SSPRK method [16] that utilizes both upwind- and downwind-biased operators. For theoretical purposes, results for the 25-step (monotonicy-preserving) extension of the $\text{TVB}_0(5,5)$ scheme are also included. Since fifth-order SSPRK methods must use downwind-biased discretizations [10,17], we have taken a fourth-order SSPRK scheme, SSPRK(5,4), as the startup procedure for all fifth-order multistep methods.

In this test we find a complete loss of stability for $\text{TVB}_0(5,5)$ at an effective CFL number of about 0.35, which about 15% larger than SSPRK(9,5) and 56% larger than eBDF5.

Surprisingly, the errors for $\text{TVB}_0(5,5)$ are noticeably larger than for the extended scheme $\text{TVB}_{\text{ext}}(25,5)$, in particular for small CFL numbers. This is because the $\text{TVB}_0(5,5)$ scheme, in combination with the fifth-order ENO discretization, generates some oscillations (the TV-increase averages 0.015 for effective CFL numbers less than 0.335) whereas the $\text{TVB}_{\text{ext}}(25,5)$ scheme does not (the TV-increase there always remains less than 3×10^{-15} for effective CFL numbers less than 0.335). An examination of the solution profiles for a sample problem (Fig. 8) illustrates that a mild oscillation forms near the rarefaction using the $\text{TVB}_0(5,5)$, but not using the $\text{TVB}_{\text{ext}}(25,5)$ scheme. We are investigating the source of this numerical behavior and note that, in general, a $\text{TVB}_0(k,p)$ scheme and its extension are expected to produce different results due to their different startup procedures. As a part of this work, we are considering improved startup procedures and methods which combine good linear and non-linear stability. Our hope is to derive simple, efficient, high-order schemes which more strictly preserve the total-variation-diminishing property.

Tests for sixth-order schemes on this Burgers problem were also carried out. The overall conclusions were quite similar to those for fifth-order: the new $\text{TVB}_0(7,6)$ and $\text{TVB}(6,6)$ gave the largest steps before producing overflow. However, in combination with sixth-order ENO discretizations, both schemes produced oscillations. Also the extension of $\text{TVB}_0(7,6)$ to a monotonicity-preserving scheme with step number 32 showed quite large errors (larger than for the lower-order results in the previous figures) so here it seems

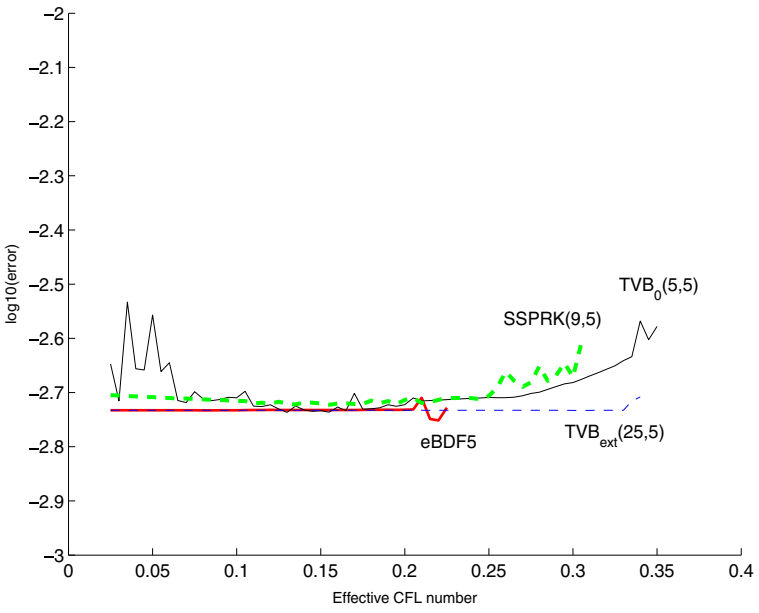

Fig. 7. Burgers' equation: L_1 errors as a function of the effective CFL number for selected fifth-order schemes.

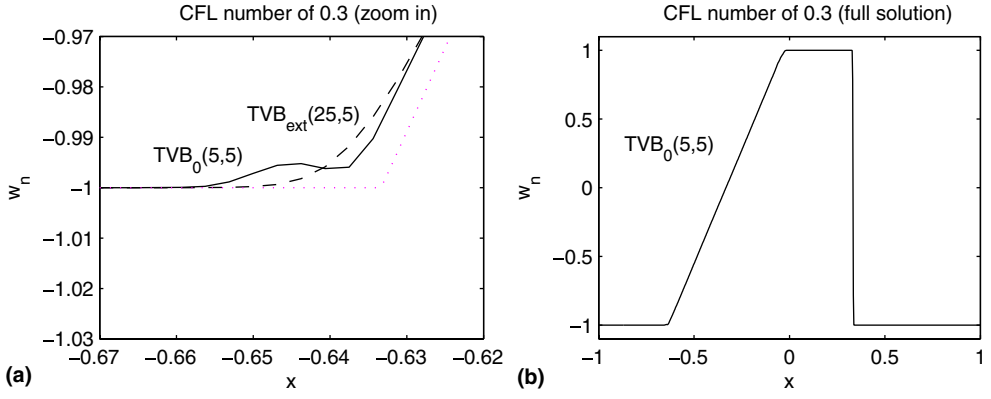

Fig. 8. Plots of the solution for fifth-order methods applied to the Burgers' equation example. (a) Zoom-in of numerical results using an effective CFL number of 0.3. eBDF5 is unstable and SSPRK(9, 5) is similar to $\mathrm{TVB}_{\mathrm{ext}}(25,5)$. (b) Global solution using an effective CFL number of 0.3.

that the combination of very high-order time stepping with the ENO discretizations is not entirely successful. Modifications and other spatial discretizations are currently under study.

Remark 4.1. The above considerations have been based on maximal CFL numbers and accuracy in the interior domain of the PDE. For many applications there are other issues that may be of importance in comparisons between Runge–Kutta and linear multistep methods.

With respect to storage requirements, the Runge–Kutta methods often have an advantage. For a general s-stage explicit Runge–Kutta method $s + 1$ registers are needed, but there are many schemes for which this

Table 9
The coefficients of the optimal monotone multistep schemes SSPMS$_+(k,p)$ with non-negative coefficients and arbitrary starting values

		$i=1$	$i=2$	$i=3$	$i=4$	$i=5$	$i=6$
SSPMS$_+(4,3)$	a_i	16/27	0	0	11/27		
$K_{LM}=1/3$	b_i	16/9	0	0	1/9		
SSPMS$_+(5,3)$	a_i	25/32	0	0	0	7/32	
$K_{LM}=1/2$	b_i	25/16	0	0	0	5/16	
SSPMS$_+(6,3)$	a_i	0.850708871672521	0.000000000000000	0.000000000000000	0.000000000000000	0.030664864534524	0.118626263792955
$K_{LM}=0.582822$	b_i	1.459638436015361	0.000000000000000	0.000000000000000	0.000000000000000	0.052614491749418	0.203537849338091
SSPMS$_+(5,4)$	a_i	0.048963857415660	0.000000000000000	0.008344481263515	0.043224046622448	0.899467614698377	
$K_{LM}=0.021190$	b_i	2.310657177903865	0.000000000000000	0.393785059936681	2.039789323347605	0.000000000000000	
SSPMS$_+(6,4)$	a_i	0.342460855717073	0.000000000000000	0.000000000000000	0.191798259434853	0.093562124938684	0.372178759909390
$K_{LM}=0.164759$	b_i	2.078553105578000	0.000000000000000	0.000000000000000	1.164112222279297	0.567871749748949	0.000000000000000

Table 10
The coefficients of the optimal monotone multistep schemes $\mathrm{SSPMS}_{\pm}(k,p)$ with downwinding and arbitrary starting values

		$i=1$	$i=2$	$i=3$	$i=4$	$i=5$	$i=6$
$\mathrm{SSPMS}_{\pm}(3,3)$	a_i	0.594610711908603	0.280806951550443	0.124582336540954			
$\tilde{K}_{\mathrm{LM}}=0.286532$	b_i	2.075197008659670	−0.980018916911766	0.434793532884448			
$\mathrm{SSPMS}_{\pm}(4,3)$	a_i	0.703966831130313	0.000000000000000	0.137026293846393	0.159006875023294		
$\tilde{K}_{\mathrm{LM}}=0.414573$	b_i	1.698053384814665	0.000000000000000	−0.330524041453602	0.383543869401605		
$\mathrm{SSPMS}_{\pm}(5,3)$	a_i	0.798493416506617	0.000000000000000	0.000000000000000	0.044490863619906	0.157015719873477	
$\tilde{K}_{\mathrm{LM}}=0.517173$	b_i	1.543958576987369	0.000000000000000	0.000000000000000	−0.086027071812365	0.303603965178621	
$\mathrm{SSPMS}_{\pm}(6,3)$	a_i	0.850708871672521	0.000000000000000	0.000000000000000	0.000000000000000	0.030664864534524	0.118626263792955
$\tilde{K}_{\mathrm{LM}}=0.582822$	b_i	1.459638436015361	0.000000000000000	0.000000000000000	0.000000000000000	0.052614491749418	0.203537849338091
$\mathrm{SSPMS}_{\pm}(4,4)$	a_i	0.397801307488879	0.289373629984981	0.258463358343857	0.054361704182283		
$\tilde{K}_{\mathrm{LM}}=0.158694$	b_i	2.506721869760679	−1.823471147931689	1.628691863739493	−0.342557126348940		
$\mathrm{SSPMS}_{\pm}(5,4)$	a_i	0.513825914465321	0.175420275745120	0.000000000000000	0.243952589290364	0.066801220499195	
$\tilde{K}_{\mathrm{LM}}=0.237094$	b_i	2.167181633581779	−0.739876267526158	0.000000000000000	1.028927417030564	−0.281749857473195	
$\mathrm{SSPMS}_{\pm}(6,4)$	a_i	0.536794943697945	0.000000000000000	0.000000000000000	0.062817026762782	0.308466977161438	0.091921052377835
$\tilde{K}_{\mathrm{LM}}=0.283199$	b_i	1.895469461211670	0.000000000000000	0.000000000000000	0.221812364797477	1.089223626016101	−0.324581201201974
$\mathrm{SSPMS}_{\pm}(5,5)$	a_i	0.250091749558196	0.255710182357537	0.325939283258897	0.138645680940752	0.029613103884618	
$\tilde{K}_{\mathrm{LM}}=0.086523$	b_i	2.890451951703556	−2.955387360726023	3.767064843589731	−1.602406635878272	0.342255408547067	
$\mathrm{SSPMS}_{\pm}(6,5)$	a_i	0.353884708765394	0.302007811177332	0.266313180919550	0.000000000000000	0.055626012991643	0.022168286146081
$\tilde{K}_{\mathrm{LM}}=0.131335$	b_i	2.694512388945229	−2.299516674862971	2.027734308798328	0.000000000000000	−0.423541841289115	0.168791474121941
$\mathrm{SSPMS}_{\pm}(6,6)$	a_i	0.149649200731278	0.202726999134910	0.327189601046664	0.214938838762387	0.091011835482769	0.014483524841992
$\tilde{K}_{\mathrm{LM}}=0.046182$	b_i	3.240407062115382	−4.389719400226429	7.084752131665459	−4.654146682007715	1.970711457151462	−0.313616885041722

can be reduced. Due to favorable combinations of method parameters, only three registers are required for the SSPRK(3, 3) method, and only four registers for the SSPRK(5, 4) method; see the Tables A.1 and A.2 in [21]. For a linear k-step method, with non-zero coefficients a_j, b_j, it natural to construct implementations that use $2k$ registers of storage. If memory considerations are important, one register can be saved by storing $(a_k w_{n-k} + \Delta t b_k F_{n-k})$ instead of w_{n-k} and F_{n-k}. Again there is a possibility of favorable combinations of coefficients, but for our optimal methods that is not the case.

Another issue that can determine the success of a method, or the failure thereof, is the accuracy near inflow boundaries of the PDE domain. Here linear multistep method have a clear advantage. Due to the fact that only approximations of order p are involved, given inflow boundary data can simply be used without degradation of accuracy. For Runge–Kutta methods on the other hand, where low-order internal approximations are used, the accuracy is often very disappointing near inflow boundaries, and to avoid that, complicated boundary corrections are needed; see, for example, [1] and Section II.2 in [8].

5. Summary and conclusions

In this paper new multistep methods are constructed that satisfy the boundedness property with optimal step size restrictions. For several cases this actually leads to methods that are monotonicity-preserving in an extended sense: there is an equivalent multistep method, with larger step number, that is monotonicity-preserving with arbitrary starting values. In general, the size of the constant M in (6) will depend on the starting procedure.

Our theoretical and numerical studies show the superiority of these new methods over the classical multistep schemes with non-negative coefficients of [19,14,3]. The new multistep methods are also more efficient in our tests than the optimal SSPRK schemes of [10,16,21].

In particular the third- and fourth-order schemes $\mathrm{TVB}_0(3,3)$, $\mathrm{TVB}(4,4)$ and $\mathrm{TVB}_0(5,4)$ gave very clear and good results. For these methods a substantial gain may be expected in situations where both monotonicity and high accuracy are sought.

For fifth- and sixth-order, theoretically optimal schemes were derived that performed very well on a linear monotonicity test. We also found that the combination of the $\mathrm{TVB}_0(5,5)$ with a fifth-order ENO spatial discretization gave good stability on a Burgers' equation example, but with some visible oscillations. Since sixth-order schemes also generated some oscillations, we continue to study fifth- and sixth-order *combinations* of spatial discretization and time stepping that are appropriate for hyperbolic conservation laws.

For many applications an order of accuracy up to four will be sufficient, and then the new bounded multistep methods are recommended in combination with the ENO discretizations. These schemes produce accurate results that are essentially free of oscillations.

Acknowledgement

We thank Nick Sahinidis for suggesting the use of product disaggregation to improve the efficiency of optimizations involving downwind-biased operators.

Appendix A. Tables of optimal monotone schemes for arbitrary starting values

In Table 9 optimal monotone schemes with non-negative coefficients are listed for number of steps up to six and order 3 and 4. Also optimal schemes with non-negative a_j and some $b_j < 0$ are listed in Table 10 for

number of steps up to six and order up to 6, complementing and improving some of the entries in [3]. See Section 2 for a discussion.

Appendix B. The proof of Theorem 2.1

The conditions on the coefficients for having order 2 are

$$\sum_{j=0}^{k-1} a_{k-j} = 1 \text{ and } \sum_{j=0}^{k-1} \left(j^q a_{k-j} + q j^{q-1} b_{k-j}\right) = k^q, \quad q = 1, 2.$$

Let $\sigma_j = \operatorname{sgn}(b_j)$ and $c_j = a_j - K|b_j|$ with $K = \tilde{K}_{\mathrm{LM}}$. Note that all $c_j \geqslant 0$. In terms of these coefficients, the order conditions can also be written as

$$\sum_{j=0}^{k-1}(c_{k-j} + K|b_{k-j}|) = 1,$$
$$\sum_{j=0}^{k-1}(jc_{k-j} + (Kj + \sigma_{k-j})|b_{k-j}|) = k,$$
$$\sum_{j=0}^{k-1}(j^2 c_{k-j} + (Kj^2 + 2\sigma_{k-j}j)|b_{k-j}|) = k^2.$$

By taking a linear combination of these relations, it is easily seen that

$$\sum_{j=0}^{k-1}(k + (k-1)j - j^2)c_{k-j} = -\sum_{j=0}^{k-1}(K(k + (k-1)j - j^2) - \sigma_{k-j}(1 - k + 2j))|b_{k-j}|.$$

All terms in the sum of the left-hand side are non-negative. Hence, at least one of the terms in the sum of the right-hand side has to be non-positive. Since $\sigma_{k-j} = \pm 1$, it follows that

$$K \leqslant \left|\frac{1 - k + 2j}{k + (k-1)j - j^2}\right|$$

for some index $0 \leqslant j \leqslant k - 1$. The maximum value is $(k-1)/k$, obtained with $j = 0, k - 1$.

References

[1] S. Abarbanel, D. Gottlieb, M.H. Carpenter, On the removal of boundary errors caused by Runge–Kutta integration of nonlinear partial differential equations, SIAM J. Sci. Comput. 17 (1996) 777–782.
[2] M. Tawarmalani, N.V. Sahinidis, Convexification and global optimization in continuous and mixed-integer nonlinear programming: theory, algorithms, software, and applications, Nonconvex Optimization and Its Applications 65, Kluwer Acdemic Publishers, Dordrecht, 2002.
[3] S. Gottlieb, C.-W. Shu, E. Tadmor, Strong stability preserving high-order time discretization methods, SIAM Rev. 42 (2001) 89–112.
[4] A. Harten, On a class of high resolution total-variation-stable finite difference schemes, SIAM J. Numer. Anal. 21 (1984) 1–23.
[5] E. Hairer, S.P. Nørsett, G. Wanner, Solving ordinary differential equations I – nonstiff problems, second ed., Springer Series in Comput. Math. 8, Springer, Berlin, 1993.
[6] W. Hundsdorfer, S.J. Ruuth, On monotonicity and boundedness properties of linear multistep methods. Math. Comput. (to appear).
[7] W. Hundsdorfer, S.J. Ruuth, R.J. Spiteri, Monotonicity-preserving linear multistep methods, SIAM J. Numer. Anal. 41 (2003) 605–623.

[8] W. Hundsdorfer, J.G. Verwer, Numerical solution of time-dependent advection–diffusion–reaction equations, Springer Series in Comput. Math. 33, Springer, Berlin, 2003.
[9] R. Jeltsch, O. Nevanlinna, Stability of explicit time discretizations for solving initial value problems, Numer. Math. 37 (1981) 61–91.
[10] J.F.B.M. Kraaijevanger, Contractivity of Runge–Kutta methods, BIT 31 (1991) 482–528.
[11] J.D. Lambert, Numerical Methods for Ordinary Differential Equations. The Initial Value Problems, Wiley, New York, 1991.
[12] C.B. Laney, Computational Gasdynamics, Cambridge University Press, Cambridge, MA, 1998.
[13] C.B. Laney, CFD Recipes: software for computational gasdynamics. Web Address: <http://capella.colorado.edu/~laney/booksoft.htm>.
[14] H.W.J. Lenferink, Contractivity preserving explicit linear multistep methods, Numer. Math. 55 (1989) 213–223.
[16] S.J. Ruuth, R.J. Spiteri, High-order strong-stability-preserving Runge–Kutta methods with downwind-biased spatial discretizations, SIAM J. Numer. Anal. 42 (3) (2004) 974–996.
[17] S.J. Ruuth, R.J. Spiteri, Two barriers on strong-stability-preserving time discretization methods, J. Sci. Comput. 17 (2002) 211–220.
[18] S.J. Ruuth, Global optimization of explicit strong-stability-preserving Runge–Kutta schemes. Math. Comput. (to appear).
[19] C.-W. Shu, Total-variation-diminishing time discretizations, SIAM J. Sci. Statist. Comput. 9 (1988) 1073–1084.
[20] C.-W. Shu, S. Osher, Efficient implementation of essentially non-oscillatory shock-capturing schemes, J. Comput. Phys. 77 (1988) 439–471.
[21] R.J. Spiteri, S.J. Ruuth, A new class of optimal high-order strong-stability-preserving time-stepping schemes, SIAM J. Numer. Anal. 40 (2002) 469–491.
[22] M. Tawarmalani, S. Ahmed, N.V. Sahinidis, Product disaggregation in global optimization and relaxations of rational programs, Optim. Eng. 3 (2002) 281–303.